Non-local magnetic field dynamics and generation

C. P. Ridgers and R. J. Kingham
Blackett Laboratory, Imperial College of Science, Technology and Medicine, London, SW7 2AZ, UK

Main contact email address **christopher.ridgers@imperial.ac.uk**

Introduction

Current interest in direct and indirect drive inertial confinement fusion (ICF) has emphasized the value of studying long-pulse laser-plasma interactions. Importantly such physics involves a significant departure from Braginskii transport theory[1] and the generation of large magnetic fields (of the order of 1MG)[2]. We must understand the interplay between these effects. Non-local transport becomes important when the collisional mean free path for electron-ion collisions of the thermal electrons is comparable to 0.01 times the scale-length of the physical variables, such as temperature, density[3]. A strong magnetic field can result in those electrons carrying most of the thermal energy – those at speeds of 2-3 times that of the thermal electrons – having gyro-radii which are smaller than their mean free paths. In this case the gyro-radius and not the collisional mean free path becomes the step-length that controls the diffusive transport. Increasing the magnetic field can reduce this step-length to a point where it is much smaller than the physical scale-lengths and so transport is localized.

In order to investigate the interplay between non-locality and magnetic field dynamics over the requisite nano-second timescales the Vlasov-Fokker-Planck (VFP) code IMPACT4 has been augmented to include hydrodynamic ion motion. IMPACT solves the VFP equation in two spatial dimensions and three velocity-space dimensions. This is made possible with current computational resources by our use of the spherical harmonic expansion to expand the distribution function in velocity space. Only the zeroth and first-order terms are retained.

Non-locality and magnetic field dynamics

The study of laser-gas jet plasma interactions in the presence of an externally applied magnetic field elucidates both the importance of non-locality[5], but also its strong coupling to the dynamics of the magnetic field and vice-versa. This was done through the simulation of the interaction of a laser with a nitrogen gas jet for 440ps in the presence of an externally applied magnetic field. The plasma conditions were chosen to match such an experiment carried out by Froula *et al.*[6]. The plasma had an electron number density of 1.5×10^{19}cm^{-3}, the laser had an intensity of 6.3×10^{14}Wcm^{-2} at 1.054μm and the imposed magnetic field was parallel to the heater beam and of strength 12T. A schematic of this experiment is shown in figure 1.

In figure 2 we see the temperature profiles after 440ps. In the case were no magnetic field was applied non-local pre-heat was observed – the hot electrons streamed out of the laser-heated region and heated the plasma ahead of the main heat front. This was suppressed by imposing a magnetic field of 12T. In the experiment the confocal length of the laser was 30mm, meaning that the beam was

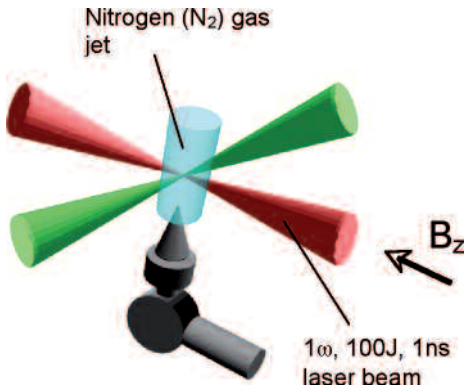

Figure 1. A schematic of experiments at LLNL using the Janus laser to investigate the effects of non-local heat transport in plasmas.

effectively cylindrical and transport along it could be neglected – we simulated the cross-field transport only. Figure 3 shows the magnetic field profile after 440ps as compared to that expected from ideal magnetohydrodynamics (iMHD). The B-field advected much more than iMHD would predict – frozen-in flow could not be the sole advection mechanism. Consider the equation for the time evolution of the magnetic field:

$$\frac{\partial B}{\partial t} + \nabla \cdot \left[\left(\mathbf{C} + \mathbf{v}_N \right) B \right] = 0 \qquad (1)$$

Resistive diffusion has been neglected in equation (1) – this is justified as the magnetic Reynolds number is of the order of 10^5. B is the z-component of the magnetic field. The velocity $\mathbf{v}_N$ is the Nernst velocity[6] and is given by $\mathbf{v}_N = 2\mathbf{q}_e/5n_eT_e$. Here, $\mathbf{q}_e$ is the heat flow, n_e is the electron number density and T_e the electron temperature. The

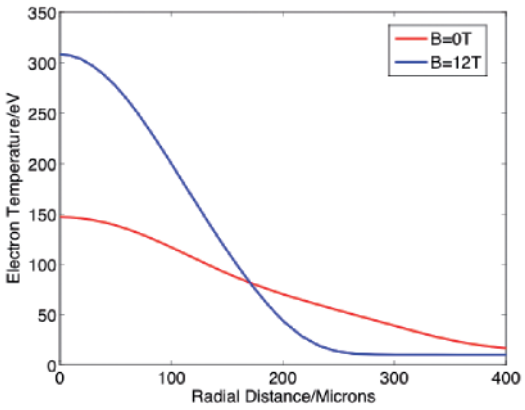

Figure 2. The temperature profiles after 440ps. The field free case is represented by the red line, the 12T case by the blue line.

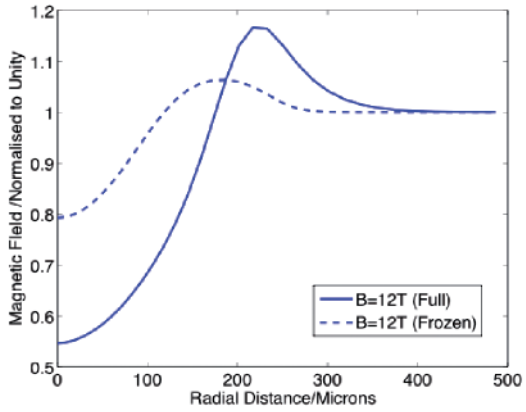

Figure 3. The magnetic field profile in the 12T case after 440ps (solid line) compared to the prediction from frozen-in flow.

Nernst effect described by this term leads to the enhanced magnetic field advection seen in the simulations. Note that equation (1) only applies when the magnetic field is perpendicular to all gradients of physical variables and the system exhibits cylindrical symmetry.

Figure 4 shows the radial heat flows for both applied field strengths. We compare these heat flows with those predicted from classical transport theory and see that non-locality is important in the field-free case. For 12T the heat flow is as predicted classically.

The distortion of the distribution function

We have shown that classical transport is inadequate to describe long-pulse laser-plasma interactions. The breakdown of classical transport is caused by two mechanisms in this case. We have discussed non-locality but it is also possible for the distribution function to be distorted away from maxwellian by inverse bremsstrahlung (IB) heating. IB causes the distribution function to tend towards super-gaussian, i.e. $f_0 \propto e^{(v/v_T)^5}$ where v_T is the electron thermal speed. We can determine which mechanism is responsible for the breakdown of classical transport by considering the distortion parameter.

$$\Delta = \frac{\langle v^{-2} \rangle}{\langle v^{-2} \rangle_M} \qquad n_e \langle v^m \rangle = 4\pi \int_0^\infty f_0 v^{m+2} dv \qquad (3)$$

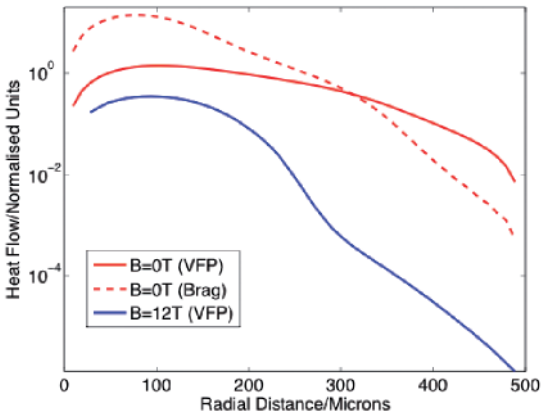

Figure 4. The radial heat flow in the field-free (red) and 12T (blue) cases as compared to Braginskii (dashed).

The subscript 'M' refers to the moment of the equivalent maxwellian distribution – i.e. one with the same number density and temperature as the plasma at that point. We can calculate this parameter analytically for a super-gaussian and we find that this results in $\Delta = 0.69$. We can also predict what the distortion parameter should be for a non-locally pre-heated region. We model the distribution function here as a two-temperature maxwellian – there is an additional hot population. In this case we predict that $\Delta = 1.05$.

The distortion parameter as calculated in the 0T and 12T cases is shown in figure 5. Also shown here is the distortion parameter when maxwellian heating (MH) was used in place of IB. This heating operator does not distort the distribution function. Non-locality was responsible for the distortion of the distribution function far from the laser-heated region and was indeed suppressed by the imposition of the 12T magnetic field. In the laser-heated region – out to 75μm from the spot's centre we see that the distortion was from IB (in the 12T case this is particularly obvious) and also from non-locality.

Magnetic field generation

In the previous simulations there was no spontaneous magnetic field generation. This was due to the cylindrical symmetry; if we relax this symmetry such generation can occur. This has been investigated by using an elliptical laser spot in the nitrogen gas jet plasma. In this case the magnetic field evolves according to:

$$\frac{\partial B}{\partial t} + \nabla \cdot \left[(\mathbf{C} + \mathbf{v}_T) B \right] = \frac{1}{n_e e} \nabla T_e \times \nabla n_e \qquad (2)$$

The generation is by the familiar thermoelectric mechanism. Figure 6 shows the field generated by an elliptical spot after 125ps. We can predict this analytically if we consider $\nabla T_e \times \nabla n_e$ for the density and temperature profiles also shown in figure 6. The density and temperature gradients were not parallel as the laser drove out more density along its minor axis – where the temperature gradient was largest. This gives rise to the peaks of the density observed.

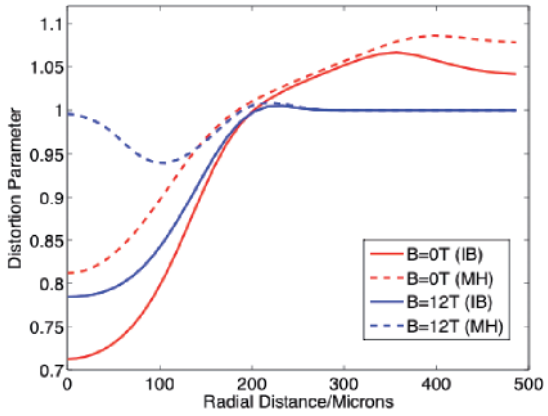

Figure 5. The distortion parameter in the field-free case (solid red line) and in the 12T case (solid blue line) using IB. The dashed lines are the same for MH.

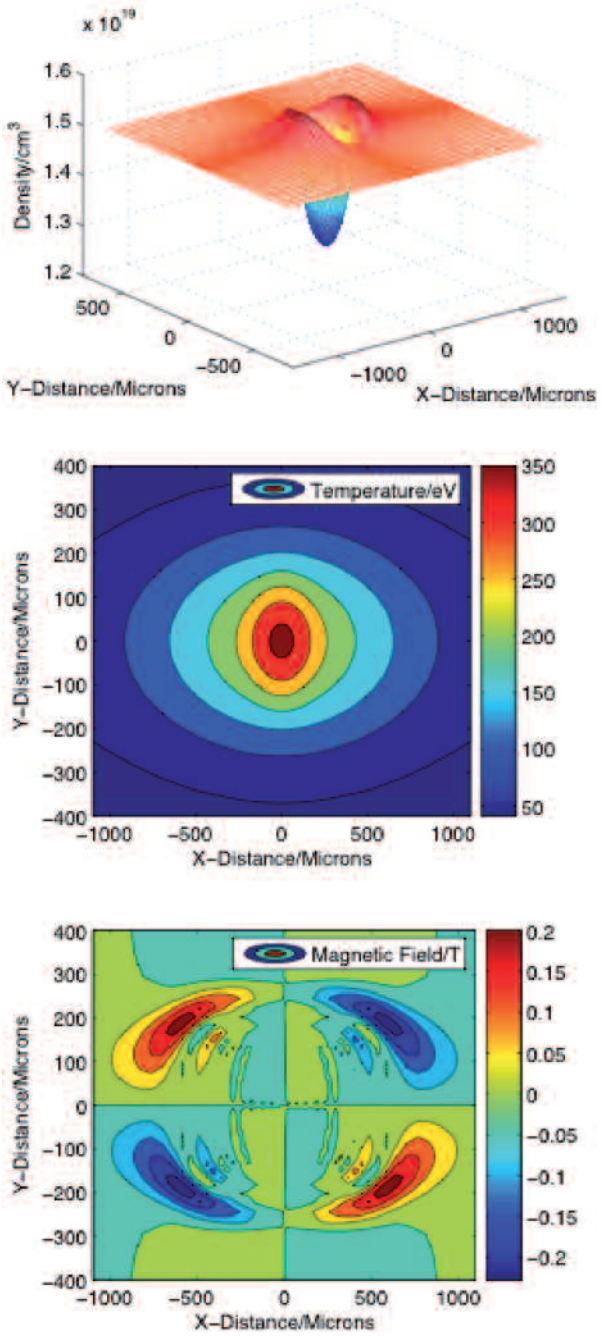

Figure 6. The results from the elliptical spot simulation after 125ps. Density profile (top), temperature profile (middle), self-generated magnetic field (bottom).

Non-local magnetic field generation

If the plasma's conditions are such that non-locality is important the theory of magnetic field generation is substantially different. The rate of change of the magnetic field is now given in terms of moments of the distribution function [7], i.e.:

$$\frac{\partial \omega}{\partial t} = \frac{\nabla\left(n_e\left\langle v^5\right\rangle\right) \times \nabla\left(n_e\left\langle v^3\right\rangle\right)}{6\left(n_e\left\langle v^3\right\rangle\right)^2} \qquad (4)$$

Such a field can be generated by an array of laser spots close to one-another. A square grid of cylindrical laser beams was simulated and generated the magnetic field shown in figure 5 about each of the spots. Classical theory predicts no B-field generation.

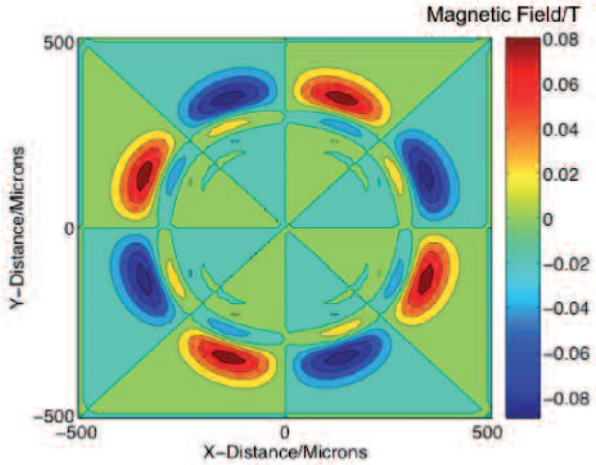

Figure 7. The magnetic field generated non-locally by a square array of circular spots after 400ps.

Acknowledgements

This work was supported by the U.K EPSRC and the Rutherford Appleton Laboratory.

References

1. S. I. Braginskii, Transport Processes in a Plasma, in *Reviews of Plasma Physics, Consultants Bureau, New York,* Vol. **1**, p. 205.
2. E. M. Epperlein and M. G. Haines, *Physics of Fluids,* Vol.**29**, No. 4, p. 1029 (1985).
3. J. A. Stamper *et al., Physical Review Letters,* Vol. **26**, No. 17, p. 1012 (1971).
4. D. R. Gray *et al., Physical Review Letters,* Vol. **39**, No. 20, p. 1270 (1977).
5. R. J. Kingham and A. Bell, *Journal of Computational Physics*, Vol. **194**, p. 1 (2004).
6. D. H. Froula *et al., Physical Review Letters,* Vol. **98**, 135001 (2007).
7. M. G. Haines, *Plasma Physics and Controlled Fusion,* Vol. **28**, p. 1705 (1986).
8. R. J. Kingham, Private Communication.